ERDC/CRREL TR-19-6

Cold Regions Research and Engineering Laboratory

US Army Corps of Engineers®
Engineer Research and Development Center

ERDC
ENGINEER RESEARCH & DEVELOPMENT CENTER

ERDC 6.2 Boreal Aspects of Ensured Maneuver (BAEM)

Physical Properties of Highly Organic Soils and Their Importance to Mobility Considerations

Susan Frankenstein and Michael W. Parker

May 2019

Physical Properties of Highly Organic Soils and Their Importance to Mobility Considerations

Susan Frankenstein and Michael W. Parker

U.S. Army Engineer Research and Development Center (ERDC)
Cold Regions Research and Engineering Laboratory (CRREL)
72 Lyme Road
Hanover, NH 03755-1290

Final Report

Prepared for Assistant Secretary of the Army for Acquisition, Logistics, and Technology
103 Army Pentagon
Washington, DC 20314-1000

Under Project 465395, ERDC 6.2 "Boreal Aspects of Ensured Maneuver (BAEM)," and Project 471941, "Remote Assessment of Snow Mechanical Properties" and "Mobility in Peat and Northern Soils"

Abstract

In this report, we begin by investigating the different methods for calculating the seasonal bearing capacity of soils, including highly organic ones such as peat. First, we present the generalized plate theories, including failure criteria, for linear elastic, plastic, and modified plastic. In all instances, the plate is assumed to be uniform, circular, and of infinite extent. The physical properties that determine soil strength change with temperature, water content, and ice content. It is therefore important to accurately predict these. Therefore, we include a section on calculating the soil thermal conductivity, which determines the flow of heat. Following the discussion on thermal conductivity, we examine existing approaches and their appropriateness to our investigation. Finally, the end of the report discusses the need for better mobility predictions in regions where seasonality is important and highly organic soils are prevalent. As part of this, we note omissions and short falls in current methods and outline how best to correct these using a combination of theory, laboratory work, and field tests.

Contents

Figures and Tables

Figures

Tables

Preface

This study was conducted for the Assistant Secretary of the Army for Acquisition, Logistics, and Technology under project number 465395, "Boreal Aspects of Ensured Maneuver (BAEM)," which is part of the U.S. Army Engineer Research and Development Center (ERDC) 6.2 Remote Assessment of Infrastructure for Ensured Maneuver (RAFTER) Program managed by Ms. Danielle Whitlow, ERDC Geotechnical and Structures Laboratory (GSL). Dr. Sally Shoop was the technical monitor. This work is continuing under project number 471941, "Remote Assessment of Snow Mechanical Properties" and "Mobility in Peat and Northern Soils," under the Entry and Sustainment in Complex Contested Environments Program managed by Dr. John Rushing, GSL.

The work was performed by the Terrestrial and Cryospheric Sciences Branch (CEERD-RRG) and the Force Projection and Sustainment Branch (CEERD-RRH) of the Research and Engineering Division (CEERD-RR), ERDC Cold Regions and Research and Engineering Laboratory (CRREL). At the time of publication, Dr. John Weatherly was Chief, CEERD-RRG; Dr. Harley Cudney was Acting Chief, CEERD-RRH; Mr. Jared Oren was Acting Chief, CEERD-RR; and Dr. Mark L. Moran was the Technical Director for military programs, CEERD-RZT. The Deputy Director of ERDC-CRREL was Mr. David B. Ringelberg, and the Director was Dr. Joseph L. Corriveau.

COL Ivan P. Beckman was Commander of ERDC, and Dr. David W. Pittman was the Director.

Acronyms and Abbreviations

CEATS	Camp Ethan Allen Training Site
CRREL	U.S. Army Cold Regions Research and Engineering Laboratory
EAFR	Ethan Allen Firing Range
ERDC	Engineer Research and Development Center
FASST	Fast All-season Soil STrength
FY	Fiscal Year
GSL	Geotechnical and Structures Laboratory
MEF	Marcell Experimental Forest
NATO	North Atlantic Treaty Organization
NRMM	NATO Reference Mobility Model
RAFTER	Remote Assessment of Infrastructure for Ensured Maneuver
SPRUCE	Spruce and Peatland Responses Under Changing Environments
USCS	Unified Soil Classification Scheme
USDA	U.S. Department of Agriculture

1 Introduction

1.1 Background

The FY16 (fiscal year 2016) Baltic Maneuver study performed by the U.S. Army Engineer Research and Development Center's Cold Regions Research and Engineering Laboratory (ERDC-CRREL) for the Night Vision and Electronic Sensor Directorate highlighted several critical gaps for maneuver capabilities against threats in northern climates. Among these are the inability to predict the strength of and mobility on highly organic soils and how these change seasonally. Terrain that is impassible in summer can become avenues of approach in winter.

Currently in NRMM (NATO [North Atlantic Treaty Organization] Reference Mobility Model), the frozen peat thickness needed to support a vehicle is determined using the method outlined by Shoop (1995). Shoop's method is based on tabular values listed by Rummukainen (1984) and Hakkarainen (1949) of recommended frozen peat thicknesses needed to support different forms of transportation commonly used by Finish foresters. These "vehicles" range from a horse to a 10-ton truck. Their lists include values for both wet and dry soils and assume that the main failure mode of the frozen peat layer is by crushing. Shoop (1995) fit two curves (wet and dry) to these values to predict the minimum frozen peat thickness needed for a specific vehicle. Inputs are the vehicle weight and whether the soil is saturated or unsaturated. If the frost depth is greater than 50 cm, there is no deflection regardless of the surface loading. Shoop (1995) notes that the uniaxial compressive strength of frozen peat is similar to other frozen soils. For non-peat soils, regardless of organic content, NRMM assumes that a frozen layer thickness of 5 cm is capable of supporting a vehicle of any size (Richmond 1991). More recent efforts studying the impact of vehicle-induced stress and displacement on frozen silt, sand, and clay (Parker et al. 2009, Coutermarsh and Shoop 2009) have found that the current NRMM approach is too conservative.

According to Parker et al. (2009), moving vehicles can adequately be modeled as static loads. They also found that when investigating soil deflection due to applied loads, the soil could be modeled as a linear elastic material.

Saarilahti (1991) argued that plasticity theory should be used when modeling vehicle bearing capacity of soils. Suvinen (2002, 2006) also found that soil deflection was best described using plasticity theory and that frost effects on soil strength could easily be incorporated if the soil was assumed to be either cohesive or frictional but not a combination of both.

1.2 Objectives

The object of this study is to highlight current practices for estimating bearing capacities, thermal conductivity, and vehicle mobility on highly organic and peat soils and to show what could be done to better predict these values.

1.3 Approach

In this report, we begin by investigating the different methods for calculating the bearing capacity of frozen soils, including peat (section 2). First, we present the generalized plate theories, including failure criteria, for linear elastic, plastic, and modified plastic. In all instances, the plate is assumed to be uniform, circular, and of infinite extent.

In section 3, we propose a new method to calculate the thermal conductivity of highly organic soils based on de Vries' (1963) and extended by Tian et al. (2016). In doing so, we first examine past approaches and compare them to our current method, which is based on Johansen (1975). Correctly quantifying how heat moves through the soil is not only important to being able to accurately predict the soil's temperature but also to determining the ice and water contents, which are important to soil strength. Section 4 follows with a discussion of ice-affected material properties.

Finally, section 5 discusses current methods to forecast vehicle mobility on highly organic and peat soils. As part of this, we note omissions and short falls and how best to correct these.

2 Bearing Capacity of Frozen Peat

2.1 Linear elastic

Much work has been done on infinite elastic plates resting on a foundation (Timoshenko and Woinowsky-Kreiger 1959; Kerr 1996; Squire et al. 1996). The plate is assumed to be thin (20 < diameter; thickness < 100), homogeneous, circular, of uniform thickness, and of infinite extent. Another critical assumption is that the deflections are small (<<thickness). Figure 1 depicts the scenario.

Figure 1. Schematic diagram of vertical forces on a circular symmetric plate.

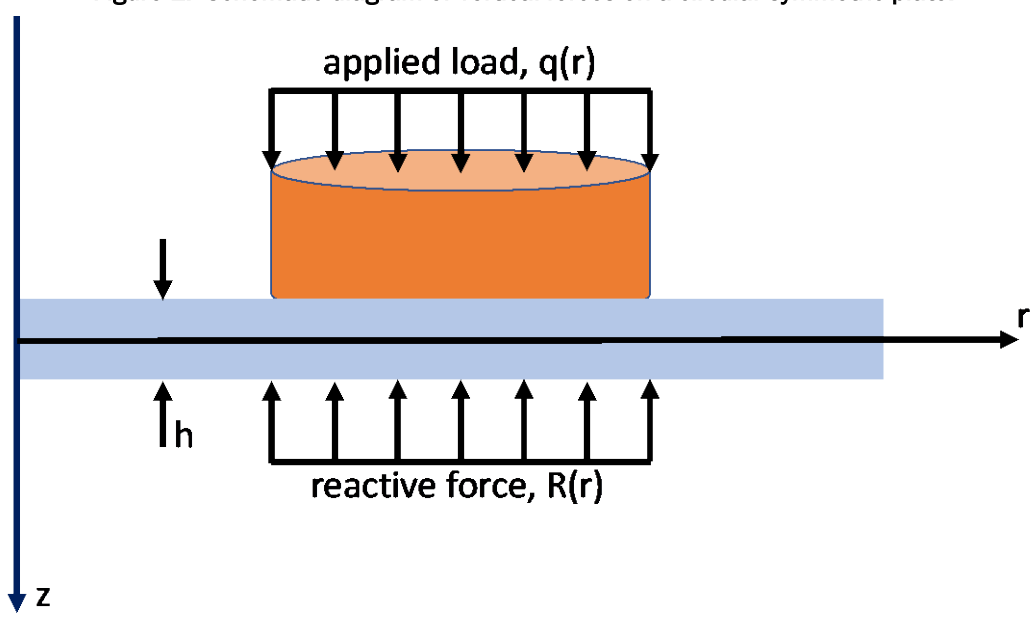

Following Timoshenko and Woinowsky-Krieger (1959) the forces, $P(r)$, on the plate are

$$P(r) = q - R = D\frac{d^4 w}{dr^4},$$
$$D = \frac{Eh^3}{12\left(1-\nu^2\right)}, \tag{1}$$

where

q = the applied load (Pa),
R = the reactive force of the foundation (Pa),
w = the displacement (m),
D = the flexural rigidity (bending stiffness) (N·m),
E = Young's modulus (Pa),
h = the thickness (m), and
ν = the Poisson ratio.

An often-used simplification is that the foundation follows Winkler's (1867) assumption that the reactive force is linearly proportional to the deflection. Thus,

$$D\frac{d^4w}{dr^4} + \rho_f g w = q\,, \tag{2}$$

where

ρ_f = the foundation density (kg/m^3) and
g = is the gravitational constant (m/s^2).

The solution to equation (2) is found in Wyman (1950) and reprinted in Squire et al. (1996). For a static point load at the center of the plate, the solution to equation (2) is

$$w = -\frac{q}{2\pi\rho_f g\lambda^2} kei\left(\frac{r}{\lambda}\right) \tag{3}$$

$\lambda = (D/\rho_f g)^{1/4}$ is the characteristic length (m) and *kei* is a zero-order Kelvin function. The maximum deflection is located at the center of the plate and is

$$w_{max} = \frac{q}{8\rho_f g\lambda^2} \tag{4}$$

since $kei(r = 0) = -\pi/4$ (Abramowitz and Stegun 1972).

For uniform circular loading, the solution to equation (2) is

$$w = \begin{cases} \dfrac{P}{\rho_f g}\left[1 + \dfrac{a}{\lambda}\left(ker'\left(\dfrac{a}{\lambda}\right)ber\left(\dfrac{r}{\lambda}\right) - kei'\left(\dfrac{a}{\lambda}\right)bei\left(\dfrac{r}{\lambda}\right)\right)\right] & 0 \le r \le a \\ \dfrac{Pa}{\rho_f g \lambda}\left[ber'\left(\dfrac{a}{\lambda}\right)ker\left(\dfrac{r}{\lambda}\right) - bei'\left(\dfrac{a}{\lambda}\right)kei\left(\dfrac{r}{\lambda}\right)\right] & r > a \end{cases} \tag{5}$$

where a is the load radius and $q = P/\pi a^2$; *ker*, *ber*, and *bei* are zero-order Kelvin functions; and *′ indicates the derivative with respect to r. The maximum again occurs at the center of the plate and is given as (Wyman 1950)

$$w_{max} = \frac{q}{\rho_f g}\left(1 + \frac{a}{\lambda} ker'\left(\frac{a}{\lambda}\right)\right) \tag{6}$$

since $ber(r = 0) = 1$ and $bei(r = 0) = 0$.

From Timoshenko and Woinowsky-Krieger (1959), the radial tensile strength (σ_r) and radial and angular bending moments (M_r, M_t) of a circular plate are

$$\begin{aligned} \sigma_r &= 6\frac{M_r}{h^2} \\ M_r &= -D\left(\frac{d^2w}{dr^2} + \frac{\nu}{r}\frac{dw}{dr}\right) \\ M_t &= -D\left(\nu\frac{d^2w}{dr^2} + \frac{1}{r}\frac{dw}{dr}\right) \end{aligned} \tag{7}$$

The maximum bending moment occurs at the center of the plate where $M_r = M_t$. Using equation (5) with $z = r/\lambda$, we have (Abramowitz and Stegun 1972)

$$
\begin{aligned}
\frac{dw}{dz} &= \frac{Pa}{\rho_f g\lambda}\left(ker'\left(\frac{a}{\lambda}\right)ber'(z) - kei'\left(\frac{a}{\lambda}\right)bei'(z)\right) \\
&= \frac{Pa}{\sqrt{2}\rho_f g\lambda}\left(ker'\left(\frac{a}{\lambda}\right)\left(ber_1(z)+bei_1(z)\right)+kei'\left(\frac{a}{\lambda}\right)\left(ber_1(z)-bei_1(z)\right)\right) \\
\frac{d^2w}{dz^2} &= \frac{Pa}{\sqrt{2}\rho_f g\lambda}\left(ker'\left(\frac{a}{\lambda}\right)\left(ber_1'(z)+bei_1'(z)\right)+kei'\left(\frac{a}{\lambda}\right)\left(ber_1'(z)-bei_1'(z)\right)\right) \\
&= \frac{Pa}{\rho_f g\lambda}\left(ker'\left(\frac{a}{\lambda}\right)\left(-\frac{1}{z}ber'(z)-bei(z)\right)+kei'\left(\frac{a}{\lambda}\right)\left(\frac{1}{z}bei'(z)-ber(z)\right)\right)
\end{aligned}
\tag{8}
$$

so that

$$
\begin{aligned}
M_r &= -D\left(\frac{d^2w}{dr^2}+\frac{\nu}{r}\frac{dw}{dr}\right) = -\frac{D}{\lambda^2}\left(\frac{d^2w}{dz^2}+\frac{\nu}{z}\frac{dw}{dz}\right) \\
&= -\frac{D}{\lambda^2}\left\{\begin{array}{l}
\dfrac{Pa}{\rho_f g\lambda}\left(\begin{array}{l} ker'\left(\dfrac{a}{\lambda}\right)\left(-\dfrac{1}{z}ber'(z)-bei(z)\right) \\ +kei'\left(\dfrac{a}{\lambda}\right)\left(\dfrac{1}{z}bei'(z)-ber(z)\right)\end{array}\right) \\
+\dfrac{\nu}{z}\dfrac{Pa}{\rho_f g\lambda}\left(ker'\left(\dfrac{a}{\lambda}\right)ber'(z)-kei'\left(\dfrac{a}{\lambda}\right)bei'(z)\right)
\end{array}\right\}.
\end{aligned}
\tag{9}
$$

The maximum stress occurs at the center of the plate where $r = 0$ ($z = 0$). Taking the limit of equation (9) using the polynomial expansions of the Kelvin functions and their derivatives (Abramowitz and Stegun 1972),

$$
\begin{aligned}
\left(M_r\right)_{max} = \lim_{z\to 0} M_r = & -\frac{PaD}{\rho_f g\lambda^3}\left(ker'\left(\frac{a}{\lambda}\right)(0-0)+kei'\left(\frac{a}{\lambda}\right)\left(\frac{1}{2}-1\right)\right) \\
& +\nu\left(ker'\left(\frac{a}{\lambda}\right)(0)-kei'\left(\frac{a}{\lambda}\right)\left(\frac{1}{2}\right)\right) \\
= & \frac{PaD}{2\rho_f g\lambda^3}(1+\nu)kei'\left(\frac{a}{\lambda}\right).
\end{aligned}
\tag{10}
$$

Rearranging equations (7) and (10), assuming $P_{cr} = \pi a^2 P$, it follows that the critical load, P_{cr}, is

$$P_{cr} = \frac{\pi a}{3(1+\nu)\lambda kei'\left(\frac{a}{\lambda}\right)} h^2 (\sigma_r)_{max} . \tag{11}$$

Equation (11) is used to determine the load needed for first crack formation. This is not necessarily the same load required for ice failure, or breakthrough. Based on experimental data for both fresh and saline ice, it is assumed that $\sigma_f > (\sigma_r)_{max}$ and $P_f > P_{cr}$, where the subscript f indicates failure. Panfilov (1960) proposed an equation of the form

$$P_f = \left(A_1 + B_1 \frac{a}{\lambda}\right) h^2 \sigma_f . \tag{12}$$

This is the form used by Shoop (1995) and Richmond et al. (1995). Their work is based on guidelines used in Finland for forest operations on peat and bog lands (Rummukainen 1984). For frost depths (h) less than 0.5 m,

$$\begin{aligned} P_f &= 0.35h^2 \quad \text{for dry soil,} \\ P_f &= 0.86h^2 \quad \text{for wet soil,} \end{aligned} \tag{13}$$

where the unit of P_f is meganewtons. Richmond et al. (1995) recommend that the dry soil version of equation (13) be used for all tracked vehicles and all wheeled vehicles weighing less than 12 tons. Also, even though equation (13) was developed for peat soils, it can be applied to other soils since the compressive strength of frozen peat is similar to other frozen mineral soils and falls within the range of frozen silts and clays (Shoop 1995).

2.2 Modified Plasticity Theory

2.2.1 The Finnish Method

The Mohr-Coulomb theory states that (Suvinen 2002)

$$\tau = c + q tan\phi , \tag{14}$$

where

τ = shear strength (kN/m²),
c = soil cohesion (kN/m²),
q = the load (kPa), and
ϕ = the soil internal friction angle (°).

The general equation for "ultimate," or critical bearing capacity (P_f, kN), for a load at the surface is based on the work of Terzaghi (1943) and is presented by (Karafiath and Nowatzki 1978) as

$$\frac{P_f}{area} = cN_c s_c i_c d_c + \gamma \frac{B}{2} N_\gamma s_\gamma i_\gamma d_\gamma , \tag{15}$$

where

c = soil cohesion (kN/m²),
γ = soil weight (kN/m³),
s_c = the shape factor for soil cohesion,
s_γ = the shape factor for soil weight,
i_c = the inclination factor for soil cohesion,
i_γ = the inclination factor for soil weight,
d_c = the depth factor for soil cohesion,
d_γ = the depth factor for soil weight,
B = t*he* load width (m),
N_c = bearing capacity factors for soil cohesion, and
N_γ = bearing capacity factors for soil weight.

N_c and N_γ depend on only the soil friction angle. The ground and the vehicle load are assumed to be flat so that $i_c = i_\gamma = 1$. For purely cohesive soils, $\phi = 0$, and for purely frictional soils, $c = 0$.

For a rectangular footing, the Terzaghi shape factors are dependent on B/L where L (m) is the load length such that equation (15) for a shallow load becomes

$$\frac{P_f}{LB} = \left[1 + 0.3\left(\frac{B}{L}\right)\right] cN_c + \left[1 - 0.2\left(\frac{B}{L}\right)\right] \gamma \frac{B}{2} N_\gamma . \tag{16}$$

For a circular load, Terzaghi found that s_c = 1.3 and s_γ = 0.6 so that equation (15) simplifies to

$$\begin{aligned}\frac{P_f}{\pi r^2} &= 1.3cN_c + 0.6\gamma\frac{2r}{2}N_\gamma \\ &= 1.3cN_c + 0.6\gamma rN_\gamma,\end{aligned} \tag{17}$$

where r (m) is the load radius. For vehicles, this is the equivalent radius of the tire contact area. If the ground is frozen, Suvinen (2006) proposes that equation (17) becomes

$$\begin{aligned}\frac{P_f}{\pi r^2} &= \left(1.3cN_c + 0.6\gamma rN_\gamma\right)\frac{B^*L^*}{BL}, \\ B^* &= B + 2h\tan\beta, \\ L^* &= L + 2h\tan\beta,\end{aligned} \tag{18}$$

where β (°) is the pressure spreading angle in the soil and h (m) is the frost depth. For vehicles, B (m) and L (m) are the width and length of the tire-soil contact area, respectively. Note that the frozen ground correction factor (B^*L^*/BL) can also be applied to equation (16). In peats, tan β = 0.9 while for mineral soils tan β = 1.0.

Suvinen (2002) and Suvinen et al. (2003) argue that soils can be categorized as either purely cohesive (ϕ = 0°) or purely frictional (c = 0). Based on that, for cohesive soils he follows the work of Skempton (1951) who quantified the ultimate load for saturated clays as

$$\begin{aligned}\frac{P_f}{area} &= cN_c \\ N_c &= \begin{cases} 6(1.2)\left(1+0.2\dfrac{D_f}{B}\right) & \text{circle} \\ 5\left(1+0.2\dfrac{B}{L}\right)\left(1+0.2\dfrac{D_f}{B}\right) & \text{rectangle}\end{cases}\end{aligned} \tag{19}$$

where D_f (m) is the depth of the footing from the surface. Even though Suvinen uses the circular shape factors in equation (17), he uses the rectangular form of N_c in equation (19). To account for freezing, Suvinen (2002,

2006) reinterprets Skempton's (1951) formulation for the cohesion factor, N_c, and critical load for cohesive soils as

$$N_c = 5\left(1+0.2\frac{B^*}{L^*}\right)\left(1+0.2\frac{h}{B^*}\right),$$
$$\left(P_f\right)_c = \pi r^2\left(1.3cN_c\right)\frac{B^*L^*}{BL}, \tag{20}$$

where D_f in equation (19) is treated as the frost depth (h). Suvinen's equation for the ultimate load for cohesive soils appears to include the shape factors twice since Skempton's (1951) quantification of N_c already includes the effect of shape. Also, there should be consistency in using either the circular or rectangular forms. Thus, for circular loads, the correct form should be

$$\left(P_f\right)_c = \pi r^2 c\left(6\left(1.2\right)\left(1+0.2\frac{h}{B^*}\right)\right)\frac{B^*L^*}{BL}. \tag{21}$$

For totally frictional soils, Suvinen (2002) follows the work of Balla (1962) so that

$$N_\gamma = 0.0488\phi^3 - 3.6055\phi^2 + 90.9482\phi - 760.7648,$$
$$\left(P_f\right)_\gamma = \pi r^2\left(0.6\gamma r N_\gamma\right)\frac{B^*L^*}{BL}. \tag{22}$$

Note that equation (22) is only valid for $20° \le \phi \le 40°$. This is not a restriction for most natural soils but could affect results for compacted terrain and highly organic ones.

For wheeled vehicles, the equivalent tire radius is (Suvinen 2002, 2006)

$$\text{contact area} = \left(\text{width}\right)^{0.8}\left(\text{diameter}\right)^{0.8}\left(\text{deflection}\right)^{0.4},$$
$$L = \frac{\text{contact area}}{\text{width}}, \tag{23}$$
$$r = \sqrt{\frac{\text{contact area}}{\pi}}.$$

The tire deflection is the difference between the loaded and unloaded wheel radii (Suvinen 2002, 2006). The above equations assume that the tire contact width is the same as the actual tire width. For tracked vehicles, the equivalent radius is calculated using (Engineering ToolBox 2003)

$$r = \frac{1}{2}\frac{1.3(BL)^{0.625}}{(B+L)^{0.25}}. \tag{24}$$

2.2.2 Modifications to the Finnish approach

The approach outlined in the previous section assumed that the soils can be classified as either granular or cohesive, allowing for simplified quantification of the bearing capacity. Very few soils, however, are either purely granular or cohesive, especially during freezing. Thus, we argue that a more general quantification of the cohesion and weight-bearing capacity factors N_c and N_γ, respectively, is needed. The method we used is that of Vesić (1973) based on the findings of Hjiaj et al. (2004). The factors are

$$\begin{aligned} N_q &= exp(\pi tan\phi)tan^2\left(\frac{\pi}{4}+\frac{\phi}{2}\right), \\ N_c &= (N_q - 1)cot\phi, \\ N_\gamma &= 2(N_q + 1)tan\phi. \end{aligned} \tag{25}$$

If the friction angle is zero, then N_c = 5.14 and N_γ = 0.0. Note that, for clayey soils, it is common practice (Fredlund and Rahardjo 1993) to calculate the stress using undrained conditions such that, N_c = 5.14.

The shape factors for rectangular loads are now

$$\begin{aligned} s_c &= 1 + \frac{N_q}{N_c}\frac{B}{L}, \\ s_\gamma &= 1 - 0.4\frac{B}{L}, \end{aligned} \tag{26}$$

and the corresponding depth factors are

$$d_c = \begin{cases} 1 + 0.4\dfrac{D_f}{B} & \dfrac{D_f}{B} \le 1 \\ 1 + 0.4 tan^{-1}\left(\dfrac{D_f}{B}\right) & \dfrac{D_f}{B} > 1 \end{cases} \tag{27}$$

$$d_\gamma = 1$$

For circular footings, B/L = 1.0. Following Suvinen's (2002, 2006) approach, the final equation for the ultimate load under freezing conditions becomes

$$\frac{P_f}{area} = \begin{cases} \left[\begin{array}{l} c\left(1 + \dfrac{N_q}{N_c}\dfrac{B^*}{L^*}\right)\left(1 + 0.4\dfrac{h}{B^*}\right)\left(N_q - 1\right)cot\,\phi \\ +\gamma B\left(1 - 0.4\dfrac{B^*}{L^*}\right)\left(N_q + 1\right)tan\,\phi \end{array} \right] \dfrac{B^* L^*}{BL} & \dfrac{h}{B} \le 1 \\ \left[\begin{array}{l} c\left(1 + \dfrac{N_q}{N_c}\dfrac{B^*}{L^*}\right)\left(1 + 0.4 tan^{-1}\left(\dfrac{h}{B^*}\right)\right)\left(N_q - 1\right)cot\,\phi \\ +\gamma B\left(1 - 0.4\dfrac{B^*}{L^*}\right)\left(N_q + 1\right)tan\,\phi \end{array} \right] \dfrac{B^* L^*}{BL} & \dfrac{h}{B} > 1 \end{cases} \tag{28}$$

As can be seen from equation (28), the strength of soil is dependent not only on its physical properties but also on predicting the temperature, water content, and ice content. The ability to move heat, or energy, through a medium depends on the thermal conductivity and heat capacity. Section 3 will discuss the best approach to model the thermal conductivity of soil, including those with high organic content. Section 4 follows with how the soil physical properties change seasonally.

3 Thermal Conductivity of Organic Soils

Many researchers have studied the thermal conductivity of soil. Farouki (1981) summarized various methods for calculating the thermal conductivity (κ) of soils, including frozen ones. All methods can be quantified as experimental, semiempirical, or empirical. Representative examples of each include Kersten (1949), de Vries (1963), and Johansen (1975), respectively.

Kersten (1949) conducted thermal conductivity measurements in the laboratory on many different Alaskan soils, including peat. As well as looking at the effects of soil mineralogy, he also investigated soil wetness and freezing. From these, he developed semiempirical equations for coarse and fine-grain soils to predict the thermal conductivity as a function of density and water content for frozen and unfrozen states. His findings, as well as the approach of de Vries (1963) discussed further below, figured heavily in Johansen's approach (1975).

3.1.1 Semiempirical methods

3.1.1.1 de Vries (1963)

de Vries' (1963) approach assumes that the soil behaves as a Maxwell-Fricke-type medium, that the particles are ellipsoidal, and that the soil sample is continuous (air or water) such that the thermal conductivity, κ, is

$$\kappa = \frac{\kappa_o f_o + \sum_{i=1}^{N} \kappa_i f_i \lambda_i}{f_o + \sum_{i=1}^{N} f_i \lambda_i}, \tag{29}$$

where

o = the soil medium, either water or air;
N = the number of particle types (sand, clay, granite, silica, etc.);
f_i = the volume fraction (m^3/m^3) of each component; and
λ_i = is a component-specific weighting, or form, factor defined as

$$\lambda_i = \frac{1}{3}\sum_{a,b,c}\left[1+\left(\frac{\kappa_i}{\kappa_0}-1\right)g_a\right]^{-1} \tag{30}$$

and $g_{a(a)} + g_{a(b)} + g_{a(c)} = 1$, where $g_{a(a,b,c)}$ are shape factors. de Vries (1963) found good agreement with experiments if $g_{a(a)} = g_{a(b)} = 0.125$ and $g_{a(c)} = 0.75$. He also found that, for dry soils, equation (29) needed to be multiplied by 1.25. Farouki (1981) realized that equation (29) could be applied to moist or unsaturated soil if the water content was above a given minimum. Farouki (1981) found that de Vries' (1963) approach could also be used for frozen soils. His version of equation (29) is

$$\begin{aligned} \kappa &= \frac{\kappa_w\theta_w + \kappa_i\theta_i\lambda_i + \left(\kappa_{air}+\kappa_{vapor}\right)f_{air}\lambda_{air} + \kappa_{soil}f_{soil}\lambda_{soil}}{\theta_w + \theta_i\lambda_{ice} + f_{air}\lambda_{air} + f_{soil}\lambda_{soil}}, \\ \kappa_{soil} &= \kappa_{quartz}^{f_{quartz}}\kappa_{other}^{1-f_{quartz}}, \end{aligned} \tag{31}$$

where θ_w and θ_i are the volumetric water and ice content (m^3/m^3), respectively. The weighting factors, equation (30), are unchanged. Farouki also used the same shape factors for both the soil and ice. The new terms needed to describe unsaturated soils are

$$\begin{aligned} &\left.\begin{aligned} \kappa_{vapor} &= \kappa_{vapor}^{sat} \\ g_{a(air)} &= 0.333-\left(0.333-0.035\right)\frac{f_{air}}{n} \end{aligned}\right\} && 0.09 \le \theta_w \le n \\ &\left.\begin{aligned} \kappa_{vapor} &= \frac{\theta_w}{0.09}\kappa_{vapor}^{sat} \\ g_{a(air)} &= 0.013+0.944\theta_w \end{aligned}\right\} && 0 \le \theta_w < 0.09 \end{aligned} \tag{32}$$

where the constants in equation (32) are those for quartz sand and n is the soil porosity.

3.1.1.2 Tian et al. (2016)

Tian et al. (2016) introduced a simplified approach to de Vries (1963) and Farouki (1981) for frozen and unfrozen soils. They assume that vapor movement is negligible and thus $\kappa_{vapor} = 0$. Further, water is the continuous medium except when $\theta_w = 0$ such that

$$
\begin{aligned}
\kappa &= \frac{\kappa_w\theta_w + \kappa_i\theta_i\lambda_i + \kappa_{air}f_{air}\lambda_{air} + \kappa_{soil}f_{soil}\lambda_{soil}}{\theta_w + \theta_i\lambda_i + f_{air}\lambda_{air} + f_{soil}\lambda_{soil}}, \\
\kappa_{dry} &= 1.25\frac{\kappa_{air}f_{air}\lambda_{air} + \kappa_{soil}f_{soil}\lambda_{soil}}{f_{air} + f_{soil}\lambda_{soil}}, \\
\kappa_{soil} &= \kappa_{sand}^{f_{sand}}\kappa_{silt}^{f_{silt}}\kappa_{clay}^{f_{clay}}, \\
g_{a(soil)} &= g_{a(sand)}f_{sand} + g_{a(silt)}f_{silt} + g_{a(clay)}f_{clay}, \\
g_{a(air)} &= 0.333\left(1 - \frac{f_{air}}{n}\right), \\
g_{a(ice)} &= 0.333\left(1 - \frac{\theta_i}{n}\right),
\end{aligned}
\tag{33}
$$

where κ_{dry} is the dry thermal conductivity. Following Johansen (1975) and others, Tian et al. (2016) assumed that $\kappa_{sand} = \kappa_{quartz} = 7.7$ W/m·K, $\kappa_{clay} = 1.93$ W/m·K, $g_{a(sand)} = g_{a(quartz)} = 0.182$, and $g_{a(clay)} = 0.00775$. The thermal conductivity and shape factors for silt are used as fitting parameters. Although Tian et al.'s (2016) approach includes freezing soils, it does not consider organics. To validate their method, Tian et al. (2016) measured the thermal conductivity of 27 different unfrozen soils and 18 frozen samples by using the heat-pulse method and values reported in the literature.

3.1.2 Empirical methods

3.1.2.1 Johansen (1975)

Johansen's method (1975) has been widely used to quantify the thermal conductivity of soils, including peat, for both frozen and unfrozen soil. As part of his thesis work investigating existing mathematical models and published experimental results, he developed an empirical method. The dependent soil properties are porosity (n), dry density (ρ_d), volumetric unfrozen water content (θ_w), volumetric ice content (θ_i), quartz content (f_{quartz}), and organic fraction (θ_{of}). Based on these, the thermal conductivity, κ (W/m·K), is

$$
\kappa = \kappa_{dry} + \left(\kappa_{sat} - \kappa_{dry}\right)K_e, \tag{34}
$$

where

$$\kappa_{dry} = \frac{135\rho_d + 64.7}{2700 - 947\rho_d} \pm 20\%, \tag{35}$$

$$\kappa_{sat} = \begin{cases} \kappa_w^n \kappa_{soil}^{(1-n)} & T > 273.15\,K \\ \kappa_w^{(n-\theta_i)} \kappa_i^{\theta_i} \kappa_{soil}^{(1-n)} & T \le 273.15\,K \end{cases}, \tag{36}$$

$$K_e = \begin{cases} 0.7 log \frac{\theta_w}{n} + 1 & T > 273.15\,K \quad coarse \\ log \frac{\theta_w}{n} + 1 & T > 273.15\,K \quad fine \\ \frac{\theta_w}{n} & T \le 273.15\,K \end{cases}, \tag{37}$$

$$\kappa_{soil} = \begin{cases} \kappa_{quartz}^{f_{quartz}} 3.0^{\left(1 - f_{quartz} - \theta_{of}\right)} \kappa_{of}^{\theta_{of}} & f_{quartz} < 0.2 \\ \kappa_{quartz}^{f_{quartz}} 2.0^{\left(1 - f_{quartz} - \theta_{of}\right)} \kappa_{of}^{\theta_{of}} & \end{cases}, \tag{38}$$

κ_{sat} is the saturated thermal conductivity, and K_e is the Kersten number, or normalized thermal conductivity. The form of the dry thermal conductivity is based on de Vries' (1963). The form of the Kersten number is based on the results of Kersten's (1949) experiments. Farouki (1981) found that Johansen's method for predicting soil thermal conductivity matched the existing data well except for the case of dry ($\theta_w/n < 0.2$), unfrozen, coarse soils.

3.1.2.2 Lu et al. (2007)

Lu et al. (2007) expanded on the Johansen (1975) and Côté and Konrad (2005) approaches. Specifically, they changed the form of the dependence of the Kersten number on the saturation ratio ($S_r = \theta_w/n$) to better represent measured values, especially for drier soils. Lu et al. (2007) also derived a new relation for the dry thermal conductivity for mineral soils. For K_e, they proposed

$$K_e = exp\left\{\alpha\left[1 - S_r^{(\alpha-\beta)}\right]\right\}, \tag{39}$$

where α depends on soil texture and the shape parameter β is 1.33 (Lu et al. 2007). Their new κ_{dry} is

$$\kappa_{dry} = -an + b\,, \tag{40}$$

where a and b are empirical parameters. Based on experiments performed on eight different soil types, Lu et al. (2007) found that, for coarse soils (sand fraction > 40%), α = 0.96; for fine grained soils, α = 0.27; and for $0.2 < n < 0.5$, a = 0.56 and b = 0.51.

3.1.3 Current approach

Both the Noah (Niu et al. 2011) and FASST (Fast All-season Soil STrength) (Frankenstein and Koenig 2004) land surface models use a modified version of Johansen's (1975) method to calculate the soil thermal conductivity to determine soil state, and hence soil strength, needed by NRMM. After a literature search, we chose the following thermal conductivity values (W/m·K) for the individual components in FAAST:

$$\begin{aligned}
\kappa_{quartz} &= 8.4 \\
\kappa_{vapour} &= 0.025 \\
\kappa_{air} &= 0.025 \\
\kappa_{water} &= 0.57 \\
\kappa_{ice} &= 2.2 \\
\kappa_{organic} &= 0.25 \\
\kappa_{non-quartz} &= 5.0 \\
\kappa_{soil} &= \frac{1}{2}\kappa_{organic}^{\theta_{of}}\kappa_{quartz}^{f_{quartz}}\kappa_{non-quartz}^{\left(1-f_{quartz}-\theta_{of}\right)}
\end{aligned}$$

Following Peters-Lidard et al. (1998), FASST assumes that the quartz content is equal to the sand fraction. For peat soils, the coarse-grained soil quantification in equation (37) is used. For sands and gravels, the method of Lu et al. (2006), equation (39), is used but with the texture and shape parameters (α and β, respectively) of Tarnawski et al. (2009) (coarse: α= 0.728, β= 1.165; fine: α= 0.37, β= 1.29).

3.1.4 New approach

We consider two approaches to predict the thermal conductivity of peat and other highly organic soils. Both begin with the method of Tian et al. (2016). For the first, a separate term for organics is added to the numerator and denominator in the top of equation (33) while for the second the soil thermal conductivity and shape factors are modified to include the organic soils, such as for the Johansen (1975) method. These two approaches are

$$\begin{aligned} \kappa &= \frac{\kappa_w\theta_w + \kappa_i\theta_i\lambda_i + \kappa_{air}f_{air}\lambda_{air} + \kappa_{soil}f_{soil}\lambda_{soil} + \kappa_{of}\theta_{of}\lambda_{of}}{\theta_w + \theta_i\lambda_i + f_{air}\lambda_{air} + f_{soil}\lambda_{soil} + \theta_{of}\lambda_{of}}, \\ \kappa_{soil} &= \kappa_{sand}^{f_{sand}}\kappa_{silt}^{f_{silt}}\kappa_{clay}^{f_{clay}}, \\ g_{a(soil)} &= g_{a(sand)}f_{sand} + g_{a(silt)}f_{silt} + g_{a(clay)}f_{clay}, \end{aligned} \tag{41}$$

and

$$\begin{aligned} \kappa &= \frac{\kappa_w\theta_w + \kappa_i\theta_i\lambda_i + \kappa_{air}f_{air}\lambda_{air} + \kappa_{soil}f_{soil}\lambda_{soil}}{\theta_w + \theta_i\lambda_i + f_{air}\lambda_{air} + f_{soil}\lambda_{soil}}, \\ \kappa_{soil} &= \kappa_{sand}^{f_{sand}}\kappa_{silt}^{f_{silt}}\kappa_{clay}^{f_{clay}}\kappa_{of}^{\theta_{of}}, \\ g_{a(soil)} &= g_{a(sand)}f_{sand} + g_{a(silt)}f_{silt} + g_{a(clay)}f_{clay} + g_{a(of)}\theta_{of}. \end{aligned} \tag{42}$$

Tian et al. (2016) suggest that $g_{a(of)} = 0.5$.

Table 1 gives volume fractions and other soil physical properties currently used by FASST for the 15 USCS (Unified Soil Classification Scheme) soil types (Frankenstein and Koenig 2004).

Typically, the organic fraction is given as a function of weight instead of volume by comparing the sample weight before and after burning off of the vegetable matter. Schaefer and Jafarov (2016) assume that the mass of carbon is 50% of the mass of organics in instances where the carbon content is known. The volume fraction of organics is $\theta_{of} = M_{of}/\Delta z\rho_{of}$ where M_{of} is the mass of the organic matter, Δz is the layer thickness, and ρ_{of} is the layer density.

Table 1. Soil default physical properties.

Soil Type	Bulk Dry Density ρ_d (g/cm³)	Porosity n	Quartz Content[7] q	Organic Fraction θ_{of}	Percent Sand f_{sand} (%)	Percent Silt f_{silt} (%)	Percent Clay f_{clay} (%)	Percent Gravel f_{gravel} (%)	Fine or Coarse
GW	1.947[2]	0.293[2]	0.65	0.00	5	2	2	91	Coarse
GP	2.079[1,2]	0.228[1,2]	0.65	0.00	5	2	2	91	Coarse
GM	1.903[2]	0.305[2]	0.65	0.05	10	12	5	68	Coarse
GC	2.133[1]	0.198[1]	0.65	0.05	10	9	31	45	Coarse
SW	1.657	0.375[3,4]	0.80	0.00	92[6]	2[6]	2[6]	4	Coarse
SP	1.643	0.375[3,4]	0.80	0.00	92[6]	2[6]	2[6]	4	Coarse
SM	1.640	0.385[3,4]	0.80	0.05	73[6,4]	15[6,4]	7[6,4]	0	Coarse
SC	1.626	0.385[3,4]	0.80	0.05	5	9	31[6,4]	0	Coarse
ML	1.458	0.453[3,4]	0.35	0.10	5	61	24[6,4]	0	Fine
CL	1.528	0.430[3,4]	0.05	0.10	5	27	58	0	Fine
OL	1.480	0.407[3,4]	0.20	0.35	5	46[6,4]	14[6,4]	0	Fine
CH	1.445	0.468[3,4]	0.05	0.10	5	28	57	0	Fine
MH	1.529	0.464[3,4]	0.35	0.10	5	61	24	0	Fine
OH	1.568	0.437[3,4]	0.20	0.25	5	16	54	0	Fine
PT	0.150	0.822[5]	0.05	0.95	1	1	3	0	Fine
SMSC (MC)*	1.658	0.384[3,4]	0.80	0.05	65[6,4]	18[6,4]	12[6,4]	0	Coarse
CLML (CM) *	1.551	0.416[3,4]	0.20	0.10	5	41	41	0	Fine

[1] Seman and Shoop (2007)
[2] Guymon et al. (1993), Table A1
[3] USDA (2018)
[4] Rollings and Rollings (1996), Table 2.11
[5] Schwärzel et al. (2006), Table 3
[6] Miller and White (1998)
[7] Tarnawski et al. (1997), pp. 96
* The two letter designation is input into the model but is not the official USCS designation.

3.1.5 Unfrozen liquid water content

The liquid water content in frozen soils is dependent on how strong the bond is between the soil particles and the water and how cold the medium is. Schaefer and Jafarov (2016) give the volumetric liquid water content under freezing conditions as a fraction of the unfrozen water content, θ_w:

$$\left(\theta_w\right)_i = \left(\frac{T_{ref} - T}{T^*}\right)^{b_i}$$
$$\theta_w = \left(1 - \theta_{of}\right)\left(f_{sand}\left(\theta_w\right)_{sand} + f_{silt}\left(\theta_w\right)_{silt} + f_{clay}\left(\theta_w\right)_{clay}\right) + \theta_{of}\left(\theta_w\right)_{of} \tag{43}$$

For pure sand, silt, clay, and organics, the reference temperature (T_{ref}) is 0.1°C; the temperature offset, T^*, is 0.01°C; and the empirical constant, b_i, is −0.9, −0.5, −0.3, and −1.0, respectively.

4 Material Properties Parameterization

As discussed in section 2, soil physical properties vary depending on water, ice content, and temperature. In this section, we present how these parameters change seasonally and due to wetting and drying events.

4.1 Shear stress

Mohr-Coulomb's law, equation (14), has been modified by researchers to account for both freezing and the degree of soil saturation. Matsushi and Matsukura (2006) included the effects of varying water content on shear strength for a sand and silt soil as

$$\tau = Ce^{-\alpha\theta_w} + \sigma' tan\phi', \tag{44}$$

where

$\sigma' = \sigma - \mu$ = the net normal stress,
μ = the pore water pressure,
θ_w = the volumetric water content,
ϕ' = the effective angle of shearing resistance,
C = the maximum cohesion, and
α = related to the susceptibility of strength reduction.

Of greater interest for this study is the effect of pore ice on shear strength. Ladanyi (2003) states that the behavior of sand and ice mixtures depends on the concentration of soil solids, $C_s = 1 - n$, where n is the porosity. If $C_s \leq 0.4$ ($n \geq 0.6$), pore ice governs behavior, while for $0.4 < C_s < 0.6$, frictional resistance between particles dominates. Finally, for $C_s \geq 0.6$ ($n \leq 0.4$), dilatancy between interlocking soil grains dictates the soil strength. Thus, assuming that the strain rate is equal to the critical one (10^{-5} h^{-1}, 2.78×10^{-9} s^{-1}),

$$\tau = \begin{cases} c(t,T) & C_s \le 0.4 \quad (n \ge 0.6) \\ \dfrac{c(t,T)}{2\sqrt{N_\phi}} + \sigma \tan\phi & C_s > 0.4 \quad (n < 0.6) \end{cases} \tag{45}$$

$$c(t,T) = \sigma_0 \left(1 + \frac{|T|}{1°C}\right)^w ,$$

where T is temperature (°C) and $c(t,T)$ is the temperature-affected cohesion. At a strain rate of 10^{-5} h^{-1} and polycrystalline ice, σ_0 = 103 kPa and w = 0.37.

4.2 Friction angle

The friction angle also changes depending on the water and ice contents. Dong et al. (2013) found that the friction angle decreased as the volumetric water content increased and fit an exponential curve to their data. As an aside, they found that roots had no effect. Yavari et al. (2016) found no relation between friction angle and temperature for temperatures above freezing for a clay and sand. They found that their results were similar to other published studies.

Arenson and Springman (2005) found for granular soils that the dependence of the friction angle on ice is

$$\phi = 32.5\left(1 - \theta_i^{2.6}\right), \tag{46}$$

where 32.5 is the unfrozen friction angle and θ_i is the volumetric ice content (0–1). Because the friction angle changes depending on the soil type, we propose a modification to equation (46):

$$\phi = \phi_u\left(1 - \theta_i^{2.6}\right), \tag{47}$$

where ϕ_u is the unfrozen friction angle for which default values are listed in Table 2. This is used to calculate the plastic weight-bearing factors N_γ, N_c, and N_q from equation (25).

Table 2. Soil parameters. Items in *pink* are considered to be cohesive in the dry state. All are for the unfrozen state.

Soil	friction angle average[1]	friction angle compacted[3]	density[2] (g/cm³)	porosity[2]	Cohesion[3] (kPa)	Cohesion compacted[3] (kPa)	Young's Modulus[4] (MPa)	Young's Modulus compacted[4] (MPa)	Poisson ratio[4]	Maximum Soil Strength, RCI[2] (psi)
GW	36.5	50	1.947	0.293	0	0	70	107	0.25	300
GP	38	50	2.079	0.228	0	0	70	107	0.25	300
GM	35	35	1.903	0.305	5	74	81.5	959	0.25	750
GC	31.5	31.5	2.133	0.198	20	50	81.5	959	0.25	750
SW	38	45	1.657	0.375	0	0	17	64.5	0.32	300
SP	34.5	37	1.643	0.375	0	0	17	64.5	0.32	300
SM	33	34	1.64	0.385	20	50	14	137.5	0.32	750
SC	35	35	1.626	0.385	5	74	14	137.5	0.25	750
ML	34	35	1.458	0.453	7	67	10	75	0.25	750
CL	31	28	1.528	0.430	4	86	15	75	0.20	750
OL	27	27	1.48	0.407	5	105	10	75	0.20	750
CH	24	19	1.445	0.468	25	103	15	75	0.25	750
MH	28	25	1.529	0.464	20	105	15	75	0.25	750
OH	26	26	1.658	0.437	10	105	10	75	0.20	750
Pt	5	5	0.15	0.822	12.5	17	0.1	0.2	0.15	300
SMSC	32.5	32.5	1.658	0.384	13.5	75	14	137.5	0.32	750
CLML	32.5	30	1.551	0.416	5.5	65	15	75	0.22	750

1 Average = 0.5*(min + max) as obtained from Geotechdata.info (2013).

2 S. Frankenstein, "User's Manual for FASST (Fast All-season Soil STrength)" (unpublished document, 2013).

3 Geotechdata.info (2014)

4 Onasch (2010)

4.3 Cohesion

Dong et al. (2013) found for low water contents that the soil cohesion increased linearly with water content but then decreased linearly after a certain point. Not enough soil types were tested to generalize the critical water content at which the transition occurs. Yavari et al. (2016) found that there was a nonlinear relation between cohesion and temperature for a clay for temperatures above freezing. Care should be taken in analyzing these results as they tested at only 5°C, 20°C, and 40°C.

4.4 Density

To compare the different approaches, the frozen states of certain physical properties are needed. Table 2 lists the unfrozen properties of 17 USCS soil types. The soil density for the frozen state is calculated as

$$\rho_{tot} = \rho_d + \rho_i n \theta_i , \tag{48}$$

where

ρ_d = the dry density (g/cm^3),
n = porosity, and
ρ_i = ice density (0.92 g/cm^3).

For compacted, on-road scenarios, we assume that the dry density increases by 10%.

4.5 Young's modulus

The frozen Young's modulus (MPa) is (Lee et al. 2002)

$$E_f = -178 + 451\rho_{tot} . \tag{49}$$

Care needs to be taken, though, when applying equation (49) to quantify the frozen Young's modulus when the soil density is lower than 0.4 g/cm^3. For most soils this is no problem, but it can be for highly organic soil.

Aukenthaler et al. (2016) assume a relation of the form

$$E_f = E_f, ref - E_{f,inc}\left(T - T_{ref}\right) \tag{50}$$

where $E_{f,ref}$ is the frozen Young's modulus at a reference temperature, T_{ref}, and $E_{f,inc}$ is the incremental change in E_f with temperature. What is unknown is whether equation (49) can be used to calculate $E_{f,\,ref}$.

4.6 Poisson ratio

The Poisson ratio is the ratio of transverse strain to axial strain or how much "thinner" something becomes when pulled from the ends. For unfrozen soils, Li and Zhao (2014) found that the Poisson ratio increased with increasing temperature. Aukenthaler et al. (2016) found a similar relation for frozen sand, silt, and clay soils in situations where there was still liquid water present in the soil matrix. When the water is totally frozen, the soil becomes rigid.

4.7 Effective soil strength

The maximum soil strength $(\sigma_r)_{max}$ (kPa) is needed for the elastic plate bending method, shown in equation (11). It is calculated as

$$\left(\sigma_r\right)_{max} = c_1\left(\sigma_s\right)_{max} + \sigma_i n\theta_i\,, \tag{51}$$

where $(\sigma_s)_{max}$ is the maximum soil strength listed in Table 2 and c_1 is a conversion factor. Since the ice strength, σ_i, varies with temperature, impurities and age, among other things, we use three representative values: 103 kPa (Ladanyi 2003), 600 kPa (Fransson 2009), and 2500 kPa (Freitag and McFadden 1997) where the lower values are used for warmer temperatures.

5 Future Studies

The previous sections have pointed out the complexity of quantifying seasonal soil strength. Some work has been done on predicting soil strength of peat soils, but the approach is inconsistent. Most of the investigations on soil physical parameters have been carried out on pure soils and do not include the effect of organics. No unifying theory exists that combines seasonal changes in inherent soil properties with soil bearing capacity, especially at the scales needed to predict vehicle mobility.

Peat and highly organic terrain, as well as gravelly soils, cover large portions of Scandinavia, the Baltic States, and the Korean peninsula; and recently, interest in these areas has increased. The current military vehicle fleet has great difficulty traversing these terrain types except under certain conditions. Therefore, there is a great need to better understand vehicle and terrain interactions in these regions to better predict vehicle mobility. Determining seasonal impacts is crucial for these areas as terrain that is impassible during warmer months can become drivable when the temperature is below freezing.

Previous studies by Wong et al. (1979, 1982) focus on unfrozen peat and muskeg for a single condition, which does not look at the effect of changing moisture conditions or the effect of freezing or thawing. Other studies conducted on multiple peat and muskeg types (Radford and Rush 1961) report general observations but do not make any correlations between vehicle mobility and peat and muskeg type. Shoop (1995) and Richmond et al. (1995) developed equation (13) to represent the breakthrough limits for a frozen peat layer over a soft substrate. It does not provide sinkage or tractive force values needed to predict vehicle mobility on this soil type.

Unlike peat and muskegs, no similar studies have been conducted on gravelly soils. In part, this is because the gravel pieces make it difficult to measure any strength-related parameters, especially in the field. Both bevemeters and traditional cone penetrometers require fairly homogeneous soils. As a result, NRMM assumes these soils to always be at maximum strength regardless of gravel or moisture content.

New experimental data sets are required to create more accurate vehicle mobility predictions across multiple seasons for highly organic and gravelly terrains. Experiments should focus on collecting vehicle mobility and

soils characterization data on both terrain types when the soil is frozen, thawed, wet, and dry to see how mobility is affected by each of these ground states. Experiments should be conducted using both tracked and wheeled vehicles if possible. Vehicle measurements should include drawbar pull, motion resistance, sinkage, wheel speed, vehicle speed, and other key parameters. These measurements should be correlated with vegetation (above and below ground) and soil temperature, moisture, density, shear strength, California bearing ratio, and other measurable parameters.

5.1 Test site selection

Three potential test sites were visited during FY18. These were Camp Ethan Allen Training Site (CEATS), Vermont; William H. Miner Agricultural Research Institute (Miner's), New York; and Marcell Experimental Forest (MEF), Minnesota. Each of these areas contain different terrain, soil, and vegetation conditions and seasonal extremes similar to Scandinavia, the Baltics, and the Korean Peninsula. Importantly, potential test sites must be vehicle accessible, fairly flat, and contain similar soils and vegetation to our areas of interest. We decided for FY19 to focus the field studies on the organic soils and to perform laboratory tests to characterize the strength of gravelly soils.

5.1.1 Camp Ethan Allen Training Site

CEATS is an 11,000-acre reserve located in northern Vermont and is home to the Army Mountain Warfare School (Figure 2). Based on the U.S. Department of Agriculture (USDA) soil map and the CEATS map, we selected three locations for possible testing. The first location is an old airstrip on the southern border that is flat and level, receives little traffic from the National Guard, and is an extensive and easily accessible space for vehicle testing (Figure 3).

The second and third locations contain taller grasses and vegetation typically found in wetter areas. While appropriate terrain conditions, they each pose slightly more difficult mobility challenges as shown in Figure 4 and Figure 5.

Figure 2. Geographic location and Topographical map of CEATS.

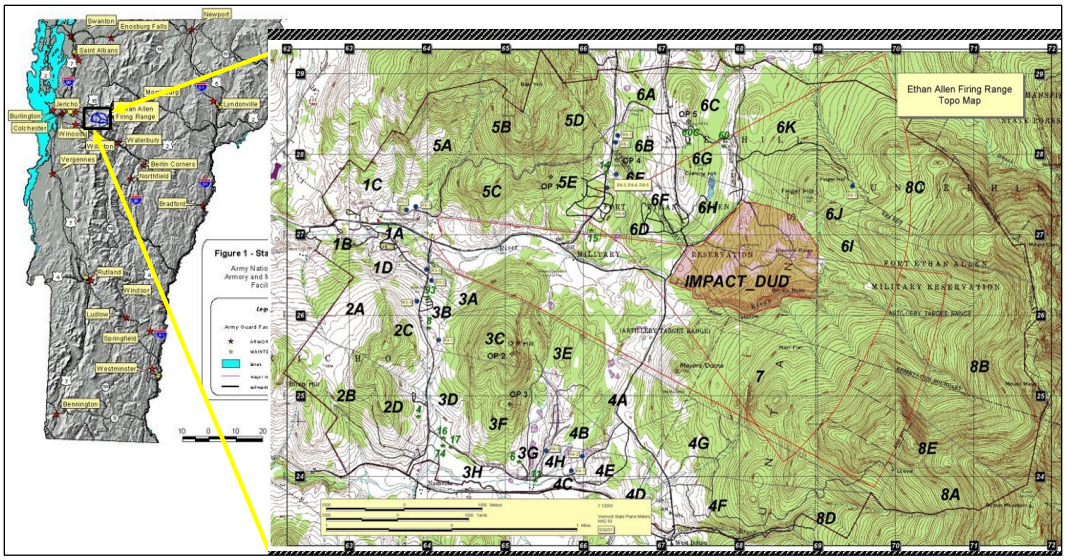

Figure 3. Old airstrip soil and terrain.

Figure 4. Range 6-3 vegetation and terrain.

Figure 5. Range 60 terrain.

5.1.2 William H. Miner Agricultural Research Institute

Miner's is a research institute located in northern New York. It contains tiled and untiled terrain, peat and highly organic soils, easily accessible terrain, and the ability to test with any vehicles necessary (Figure 6). Miner's is located in close proximity to EAFR, allowing experimental testing to be combined between the two facilities. This will shorten test events and will allow researchers and vehicles to travel between sites with minimal logistics required for moving equipment and test vehicles.

Figure 6. Miner's soil and terrain.

5.1.3 Marcell Experimental Forest

MEF is located in northern Minnesota and falls under the jurisdiction of the USDA Forrest Service, Northern Research Station. It is home to the Spruce and Peatland Responses Under Changing Environments (SPRUCE) experiment. This is a multi-organization, 10-year experiment to measure the effects of warming and increased CO_2 on the peatland ecosystem. It is funded primarily by the U.S. Department of Energy and currently hosts in excess of 50 experiments. This and other studies by the University of Minnesota and the Minnesota research council at MEF provide a wide variety of current and historical measurements of the environment and seasonal soil conditions that will supplement data collected by any vehicle experiments. These groups share a common interest with CRREL in that they are also interested in vehicle mobility on peatlands to identify when they will support logging operations without causing destruction of the environment.

There are several sites at MEF with peat bogs and fens that provide unique sites for vehicle mobility research. We visited several of these in June 2018. These sites include Jennies Bog, Junction Fen (Figure 7), S7, Bog Lake Fen (Figure 8), and other unnamed locations. Each of these sites requires that vehicle testing occur in the winter only when the ground is frozen. The ground is too wet any other time of year; and the vehicles will become mired, causing large soil disturbances and likely immobilizing the

test vehicles. Junction Fen and Bog Lake Fen are the only ones feasible for vehicle testing as the others are too heavily vegetated or are inaccessible without major tree clearing.

Figure 7. *Left*, Junction Fen, showing temperature probe (*center*) and snow course markers (*posts*); *right*, Junction Fen grasses, sphagnum moss, and sun dew.

Figure 8. Bog Lake Fen, showing sparse trees and instrumentation.

Junction Fen is the best location for conducting vehicle mobility research and currently has a snow course across the fen where depth and density are measured annually, on-site power, and a temperature probe down to 2 m with measurements since the 1980s. It has almost no trees but does have small hillocks 25–75 cm high. The low vegetation includes leather leaf, grasses, sphagnum moss, pitcher plants, and sun dew. The peat thickness near the middle of the fen is approximately 3 m and is sapric (muck, contains less than one-sixth fibers by volume).

5.2 Field testing

Testing is currently scheduled to be conducted at EAFR and Miner's during FY19 because of the close proximity to CRREL and currently established permissions to conduct vehicle testing. Testing at MEF requires additional environmental permissions that will be pursued in FY19 in anticipation of FY20 field testing. Vehicle mobility testing will be conducted with an instrumented wheeled vehicle and a lightweight tracked vehicle (if available).

6 Conclusions

In this report we began by discussing different methods for calculating the bearing capacity of soils, including highly organic and gravelly ones. This was followed by a treatise of how the physical properties needed to determine the strength of soil change with temperature, water, and ice content. Next, we investigated the different approaches used to predict heat flow through soils and how these needed to be modified for organic soils. Finally, we presented the groundwork undertaken thus far to develop field and laboratory testing plans with which to validate the new methodology presented in this document as it relates to seasonal cross-country vehicle mobility.

References

Abramowitz, M., and I. A. Stegun. 1972. *Handbook of Mathematical Functions with Formulas, Graphs, and Mathematical Tables*. New York: Dover Publishing, Inc.

Arenson, L. U., and S. M. Springman. 2005. "Mathematical Descriptions for the Behavior of Ice-Rich Frozen Soils at Temperatures Close to 0°C." *Canadian Geotechnical Journal* 42:431–442.

Aukenthaler, M., R. B. J. Brinkgreve, and A. Haxaire. 2016. "Evaluation and Application of a Constitutive Model for Frozen and Unfrozen Soil." In *Proceedings, GeoVancouver 2016: the 69th Canadian Geotechnical Conference*, Vancouver, Canada, 1–8.

Balla, A. 1962. "Bearing Capacity of foundations." *Journal of the Soil Mechanics and Foundations Division, ASCE* 89 (SM5): 13–34.

Côté, J., and J.-M. Konrad. 2005. "A Generalized Thermal Conductivity Model for Soils and Construction Materials." *Canadian Geotechnical Journal* 42:443–458.

Coutermarsh, B., and S. Shoop. 2009. "Modeling Wheel Loading on Frozen Ground." In *Proceedings, 16th International Conference of the International Society for Terrain-Vehicle Systems,* Turin, Italy, 25–28 November.

de Vries, D. A. 1963. "Thermal Properties of Soils." In *Physics of Plant Environment*, W. R. van Wijk, ed., 210–235. New York: John Wiley & Sons.

Dong, Y., Y. Uw, J. Yin, Y. Wang, and S. Gou. 2013. "Investigation of Soil Shear-Strength Parameters and Prediction of the Collapse of Gully Walls in the Black Soil Region of Northeastern China." *Physical Geography* 32(2).

Engineering ToolBox. 2003. "Hydraulic Diameter." Engineering ToolBox. https://www.engineeringtoolbox.com/hydraulic-equivalent-diameter-d_458.html.

Farouki, O. T. 1981. *Thermal Properties of Soils*. Monograph 81-1. Hanover, NH: U.S. Army Cold Regions Research and Engineering Laboratory.

Frankenstein, S., and G. G. Koenig. 2004. *Fast All-season Soil STrength (FASST)*. ERDC/CRREL SR-04-1. Hanover, NH: U.S. Army Engineer Research and Development Center. http://hdl.handle.net/11681/11814.

Fransson, L. 2009. *Ice Handbook for Engineers, V. 1.2*. 2009-01-29. Luleå, Sweden: Luleå University of Technology.

Fredlund, D. G., and H. Rahardjo. 1993. *Soil Mechanics for Unsaturated Soils*. New York: John Wiley & Sons.

Freitag, D. R., and T. McFadden. 1997. *Introduction to Cold Regions Engineering*. New York: ASCE Press.

Geotechdata.info. 2013. "Soil Friction Angle." Geotechdata.info. Updated 14 December 2013. http://www.geotechdata.info/parameter/angle-of-friction.html.

Geotechdata.info. 2014. "Soil Cohesion." Geotechdata.info. Updated 31 October 2014. http://www.geotechdata.info/parameter/cohesion.html.

Guymon, G. L., R. L. Berg, and T. V. Hromadka. 1993. *Mathematical Model of Frost Heave and Thaw Settlement in Pavements*. CRREL Report 93-2. Hanover, NH: U.S. Army Cold Regions Research and Engineering Laboratory.

Hakkarainen, A. 1949. "Routa talviteiden rakentajana." [In Finnish.] *Metsätehon tiedotus* 29.

Hjiaj, M., A. V. Lyamin, and S. W. Sloan. 2004. "Bearing Capacity of a Cohesive-Frictional Soil under Non-Eccentric Inclined Loading." *Computers and Geotechnics* 31:491–516.

Johansen, O. 1975. Thermal Conductivity of Soils. Ph.D. thesis, Trondheim, Norway. Draft Translation 637, 1977. Hanover, NH: U.S. Army Cold Regions Research and Engineering Laboratory.

Karafiath, L. L., and E. A. Nowatzki. 1978. *Soil Mechanics for Off-Road Vehicle Engineering*. Clausthal, Gemany: Trans Tech Publications.

Kerr, A. D. 1996. "Bearing Capacity of Floating Ice Covers Subjected to Static, Moving, and Oscillatory Loads." *Applied Mechanics Reviews* 49 (11): 463–476.

Kersten, M. S. 1949. *Thermal Properties of Soils*. Bulletin No. 28. Minneapolis, MN: University of Minnesota. http://hdl.handle.net/11299/124271.

Ladanyi, B. 2003. "Rheology of Ice/Rock Systems and Interfaces." In *Proceedings, 8th International Conference on Permafrost*, 21–25 July, Zurich, Switzerland, ed. M. Phillips, S. Springman, and L. Arenson, 621–626.

Lee, M. Y., A. Fossum, L. S. Costin, and D. Bronowski. 2002. *Frozen Soil Material Testing and Constitutive Modeling*. Sandia Report SAND2002-0524. Albuquerque, NM: Sandia National Laboratories.

Li, M., and Y. Zhao. 2014. "Prestack Seismic Inversion and Seismic Attribute Analysis." In *Geophysical Exploration Technology: Applications in Lithological and Stratigraphic Resources*, 199-219. Waltham, MA: Elsevier

Lu, S., T. Ren, Y. Gong, and R. Horton. 2007. "An Improved Model for Predicting Soil Thermal Conductivity from Water Content at Room Temperature." *Soil Science Society of America Journal* 71 (1): 8–14.

Matsushi, Y., and Y. Matsukura. 2006. "Cohesion of Unsaturated Residual Soils as a Function of Volumetric Water Content." *Bulletin of Engineering Geology and the Environment* 65:449–455.

Miller, D. A., and R. A. White. 1998. "A Conterminous United States Multi-Layer Soil Characteristics Data Set for Regional Climate and Hydrology Modeling." *Earth Interactions* 2:1–26. https://doi.org/10.1175/1087-3562(1998)002<0001:ACUSMS>2.3.CO;2.

Niu, G.-Y., Z.-L. Yang, K. E. Mitchell, F. Chen, M. B. Ek, M. Barlage, L. Longuevergne, A. Kumar, K. Manning, D. Niyogi, E. Rosero, M. Tewari, and Y. Xia. 2011. "The Community Noah Land Surface Model with Multiparameterization Options (Noah-MP): 1. Model Description and Evaluation with Local-Scale Measurements." *Journal of Geophysical Research* 116 (D12109). https://doi.org/10.1029/2010JD015139.

Onasch, C. 2010. Some Useful Numbers on the Engineering Properties of Materials (Geologic and Otherwise). https://www.jsg.utexas.edu/tyzhu/files/Some-Useful-Numbers.pdf.

Panfilov, D. F. 1960. "Experimental Investigation of the Carrying Capacity of a Floating Ice Plate." [In Russian]. *Izvestia Vsesojuznogo Nauchno-Issledovatelskogo Instituta Gidrotekhniki* 64:101–115.

Parker, M., B. Coutermarsh, and S. Shoop. 2009. "Modeling Heavy Wheel Loading on Frozen and Unfrozen Ground." In *Proceedings, ASCE 14th Conference on Cold Regions Engineering*, 20 August–2 September, Duluth, MN.

Peters-Lidard, C. D., E. Blackburn, X. Liang, and E. F. Wood. 1998. "The Effect of Soil Thermal Conductivity Parameterization on Surface Energy Fluxes and Temperature." *Journal of Atmospheric Sciences* 55:1209–1224.

Radforth, N., and E. Rush. 1961. *Trafficability Tests on Confined Organic Terrain (Muskeg). Report 1: Summer 1961 Tests*. Technical Report, No.3-656. Vicksburg, MS: Waterways Experimentation Station.

Richmond, P. W. 1991. *Notes for Cold Weather Military Operations*. CRREL Special Report 91-30. Hanover, NH: U.S. Army Cold Regions Research and Engineering Laboratory.

Richmond, P. W., S. A. Shoop, and G. L. Blaisdell. 1995. *Cold Regions Mobility Models*. CRREL Report 95-1. Hanover, NH: U.S. Army Cold Regions Research and Engineering Laboratory. http://hdl.handle.net/11681/9179.

Rollings, M. P., and R. S. Rollings, Jr. 1996. *Geotechnical Materials in Construction*. New York: McGraw-Hill.

Rummukainen, A. 1984. *Peatland Properties and Their Evaluation for Wood Harvesting*. Final Report for "Harvesting on Peatlands," Nordic Research Council on Forest Operations (NSR), 1977–1983. Research Notes 45. Helsinki: University of Helsinki, Department of Logging and Utilization of Forest Products.

Saarilahti, M., 1991. "Maastoliikkuvuuden perusteet." [In Finnish.] *Metsäntutkimuslaitoksen tiedonantoja* 390.

Schaefer, K., and E. Jafarov. 2016. "A Parameterization of Respiration in Frozen Soils Based on Substrate Availability." *Biogeosciences* 13:1991–2001.

Schwärzel, K., J. Šimůnek, H. Stoffregen, G. Wessolek, and M. Th. Van Genuchten. 2006. "Estimation of the Unsaturated Hydraulic Conductivity of Peat Soils: Laboratory versus Field Data." *Vadose Zone Journal* 5:628–640.

Seman, P. M., and S. A. Shoop. 2007. *In Situ California Bearing Ratio Database*. ERDC/CRREL TR-07-21. Hanover, NH: U.S. Army Engineer Research and Development Center.

Shoop, S., 1995. "Vehicle Bearing Capacity of Frozen Ground over a Soft Substrate." *Canadian Geotechnical Journal* 32:552–556.

Skempton, A. W. 1951. "The Bearing Capacity of Clays." In P*roceedings, Building Research Congress*, 1:180–189.

Squire, V., R. J. Hosking, A. D. Kerr, and P. J. Langhorne. 1996. *Moving Loads on Ice Plates*. Dordrecht, The Netherlands: Kluwer Academic Publishers.

Suvinen, A., 2002. Terrain Mobility Model and Determination of Optimal Off-Road Route. Thesis, University of Helsinki. http://hdl.handle.net/1975/8066.

———. 2006. "A GIS-Based Simulation Model for Terrain Tractablility." *Journal of Terramechnics* 43:427–449.

Suvinen, A., M. Saarilahti, and T. Tokola. 2003. "Terrain Mobility Model and Determination of Optimal Off-Road Route." In *Proceedings, 9th Scandinavian Research Conference on Geographical Information Science, ScanGIS 2003*, 4–6 June, Espoo, Finland, 251–259.

Tarnawski, V. R., B. Wagner, J. Webber, and L. Pettipas. 1997. "Optimization of Soil Mineralogical Composition for Prediction Soil Thermal Conductivity." In *Proceedings of the International Symposium on Physics, Chemistry, and Ecology of Seasonally Frozen Soils, Fairbanks, AK, June 10–12*, ed. I. K. Iskandar, E. A. Wright, J. K. Radke, B. S. Sharratt, P. H. Groenevelt, L. D. Hinzman, 91–97. Special Report 97-10. Hanover, NH: U.S. Army Cold Regions Research and Engineering Laboratory.

Tarnawski, V. R., T. Momose, and W. H. Leong. 2009. "Assessing the Impact of Quartz Content on the Prediction of Soil Thermal Conductivity." *Géotechnique* 59 (4): 331–338.

Terzaghi, K. 1943. *Theoretical Soil Mechanics*. New York: John Wiley & Sons, Inc.

Tian, Z., Y. Lu, R. Horton, and T. Ren. 2016. "A Simplified de Vries-Based Model to Estimate Thermal Conductivity of Unfrozen and Frozen Soil." *European Journal of Soil Science* 67:564–572.

Timoshenko, S., and W. Woinowsky-Krieger. 1959. *Theory of Plates and Shells*. New York: McGraw-Hill.

USDA (U.S. Department of Agriculture). 2018. "ROSETTA Class Average Hydraulic Parameters." U.S. Salinity Laboratory: Riverside, CA. http://www.ars.usda.gov/Services/docs.htm?docid=8955.

Vesić, A. 1973. "Analysis of Ultimate Loads of Shallow Foundations." *Journal of the Soil Mechanics and Foundations Division* 99 (SM1): 45–73.

Winkler, E., 1867. "Die Lehre von der Elastizität und Festigkeit." [In German.] Prauge: Verlag von H. Dominicus.

Wong, J., M. Garber, J. Radforth, and J. Dowell. 1979. "Characterization of the Mechanical Properties of Muskeg with Special Reference to Vehicle Mobility." *Journal of Terramechanics* 16 (4): 163–180.

Wong, J., J. Radforth, and J. Preston-Thomas. 1982. "Some Further Studies on the Mechanical Properties of Muskeg in Relation to Vehicle Mobility." *Journal of Terramechanics* 19 (2): 107–127.

Wyman, M. 1950. "Deflections of an Infinite Plate." *Canadian Journal of Research* 28 (A): 293–302.

Yavari, N., A. Minh Tang, J.-M. Pereira, and G. Hassen. 2016. "Effect of Temperature on the Shear Strength of Soils and the Soil-Structure Interface." *Canadian Geotechnical Journal* 53 (7): 1186–1194.

REPORT DOCUMENTATION PAGE

Form Approved
OMB No. 0704-0188

1. REPORT DATE *(DD-MM-YYYY)*
May 2019

2. REPORT TYPE
Technical Report/Final

3. DATES COVERED *(From - To)*

4. TITLE AND SUBTITLE
Physical Properties of Highly Organic Soils and Their Importance to Mobility Considerations

5a. CONTRACT NUMBER

5b. GRANT NUMBER

5c. PROGRAM ELEMENT NUMBER

6. AUTHOR(S)
Susan Frankenstein and Michael W. Parker

5d. PROJECT NUMBER
465395 & 471941

5e. TASK NUMBER

5f. WORK UNIT NUMBER

7. PERFORMING ORGANIZATION NAME(S) AND ADDRESS(ES)
U.S. Army Engineer Research and Development Center (ERDC)
Cold Regions Research and Engineering Laboratory (CRREL)
72 Lyme Road
Hanover, NH 03755-1290

8. PERFORMING ORGANIZATION REPORT NUMBER
ERDC/CRREL TR-19-6

9. SPONSORING / MONITORING AGENCY NAME(S) AND ADDRESS(ES)
Assistant Secretary of the Army for Acquisition, Logistics, and Technology
103 Army Pentagon
Washington, DC 20314-1000

10. SPONSOR/MONITOR'S ACRONYM(S)
ASA(ALT)

11. SPONSOR/MONITOR'S REPORT NUMBER(S)

12. DISTRIBUTION / AVAILABILITY STATEMENT
Approved for public release; distribution is unlimited.

13. SUPPLEMENTARY NOTES
ERDC 6.2 Boreal Aspects of Ensured Maneuver (BAEM)

14. ABSTRACT

In this report, we begin by investigating the different methods for calculating the seasonal bearing capacity of soils, including highly organic ones such as peat. First, we present the generalized plate theories, including failure criteria, for linear elastic, plastic, and modified plastic. In all instances, the plate is assumed to be uniform, circular, and of infinite extent. The physical properties that determine soil strength change with temperature, water content, and ice content. It is therefore important to accurately predict these. Therefore, we include a section on calculating the soil thermal conductivity, which determines the flow of heat. Following the discussion on thermal conductivity, we examine existing approaches and their appropriateness to our investigation. Finally, the end of the report discusses the need for better mobility predictions in regions where seasonality is important and highly organic soils are prevalent. As part of this, we note omissions and short falls in current methods and outline how best to correct these using a combination of theory, laboratory work, and field tests.

15. SUBJECT TERMS
Mobility, Organic soils, Physical properties, Seasonal, Shear strength of soils, Soil mechanics, Trafficability

16. SECURITY CLASSIFICATION OF:			17. LIMITATION OF ABSTRACT	18. NUMBER OF PAGES	19a. NAME OF RESPONSIBLE PERSON
a. REPORT	b. ABSTRACT	c. THIS PAGE			19b. TELEPHONE NUMBER *(include area code)*
Unclassified	Unclassified	Unclassified	SAR	45	